UCD: 539.216:546.817:548.736.442.6 doi: 10.33609/2708-129X.88.04.2022.79-93

INFLUENCE OF THE SOLVENT AND THE RATIO OF STARTING REAGENTS ON THE PROPERTIES OF ORGANIC-INORGANIC PEROVSKITE MAPbI$_3$

Torchyniuk P.V.[1], V'yunov O.I.*[1], Vlasiuk V.M.[2], Kostylyov V.P.[2], Belous A.G.[1]

[1]V.I. Vernadsky Institute of General and Inorganic Chemistry of National Academy of Sciences of Ukraine, Acad. Palladina Ave., 32/34, Kyiv 03142, Ukraine
[2]V.E. Lashkarev Institute of Semiconductor Physics of National Academy of Sciences of Ukraine, pr. Nauki 41, Kyiv 03028, Ukraine
** e-mail: vyunov@ionc.kiev.ua*

The peculiarities of formation and properties of organic-inorganic MAPbI$_3$ perovskite films, obtained from solutions with different ratios of starting reagents (PbI$_2$:MAI = 1:1,1:2, and 1:3), in the DMF and DMSO solvents, studied. As the PbI$_2$:MAI ratio increases, the temperature of the formation of a single-phase MAPbI$_3$ perovskite film also increases. The slight changes in the structural and electrophysical characteristics for perovskite films obtained at the different ratios of PbI$_2$:MAI in DMF and DMSO were found. These changes are related to the solvent that is included in the crystalline structure of perovskite. In the same ratios of starting reagents, DMF is included in the structure of perovskite in a greater amount than DMSO.

Keywords: organic-inorganic perovskite, phase transformations, structural parameters, electrophysical characteristics.

INTRODUCTION. The global energy crisis is one of the greatest challenges facing humanity. It is necessary to develop new technologies for the successful use of energy from renewable sources due to the reduced availability of fossil fuels. Solar energy is a rich, freely available source and promising replacement for non-renewable fossil fuels.

The solar cells based on organic-inorganic perovskites have attracted the attention of scientists according to a significant increase in efficiency to 25.2%, low cost, and ease of production. [1–2]. This effect was achieved by improving the design of solar cells, adding new conductive layers (of n- and p-type), and improving the quality of the perovskite films. Organic-inorganic perovskites combine the advantages of organic and inorganic semiconductors: high optical absorption, high mobility of charge carriers [3], and regulated bandgap [4].

Photoactive halide perovskites usually exhibit a three-dimensional crystal structure with the characteristic chemical formula ABX$_3$, where A is a monovalent cation of methylammonium ($CH_3NH_3^+$), formamidinium ($HC(NH_2)_2^+$), cesium (Cs^+) or rubidium (Rb^+), and B is a divalent metal cation Pb^{2+} or Sn^{2+}, and X is a halide anion (Cl^-, Br^- or I^-) [5, 6].

Achieving the high photoelectric characteristics of organic-inorganic perovskite depends on the nucleation and growth of crystal processes. As a result of the process control, it is possible to obtain a smooth and compact film of perovskite. External factors (temperature, moisture, oxygen), as well as solvent, methods of obtaining films, and annealing can significantly affect the structural and physical properties of organic-inorganic perovskite. It is known that solvents (DMF, DMSO, γ-butyrolactone (GBL), NMP) [7, 8] were used for the synthesis of perovskites can affect the properties of films.

Changes in the synthesis conditions (ratio of starting reagents and solvent) may affect the properties of perovskites. It was shown that the ratio of starting reagents PbI_2:MAI (CH_3NH_3I) affects electrophysical characteristics, particularly, the bandgap [9]. Solvent replacement also affects the properties of organic-inorganic perovskite. An increase in the stability of films to moisture and the mobility of charge carriers detected by using dimethyl sulfoxide instead of dimethylformamide during the synthesis of perovskite [10].

The method of obtaining perovskites is a key factor in achieving high characteristics (surface coverage, crystallinity, thickness, and quality of films responsible for the morphological and transport properties of perovskite). Several methods can be used to obtain films of organic-inorganic perovskites. The most common methods of them are one-step and two-step deposition, spin-coating, the method of rapid deposition crystallization, and thermal evaporation.

It is known that organic-inorganic perovskites are unstable materials that can degrade and decompose into various components under the influence of external factors. Finding ways to increase the stability of perovskites is an urgent task, as its solution will allow them to be used in the large-scale creation of solar cells. Nowadays, the best laboratory samples of elements based on perovskite demonstrate high efficiency and a low cost of their production. However, they have relatively low stability, although some solar cells show stable operation throughout the year [11, 12].

This work aims to study the peculiarities of perovskite formation, and structural and electrophysical characteristics of organic-inorganic $MAPbI_3$ perovskite films depending on the solvent and the ratio of starting reagents.

EXPERIMENT AND DISCUSSION OF THE RESULTS.

Materials. Lead iodide (PbI_2) and methylammonium iodide MAI (CH_3NH_3I) were used as starting reagents for the synthesis of organic-inorganic perovskites. To stabilize the structure of perovskite, partial replacement of iodine with chlorine was carried out by adding chemically pure methylammonium chloride MACl (CH_3NH_3Cl). Dried chemically pure dimethylformamide (DMF) and dimethyl sulfoxide (DMSO) were used as solvents.

The starting reagents PbI_2 and MAI in the ratios 1:1, 1:2, 1:3 were dissolved in DMF and DMSO and stirred at 70 °C for 1 hour to obtain $MAPbI_3$ ($CH_3NH_3PbI_3$) films. The formation of crystalline $MAPbI_3$ films was performed in a dry box. A pre-prepared clear solution was deposited on cleaned glass substrates by spin-coating at a speed of 1200 rpm for 30 s. The heat treatment of the films was performed on a preheated stove at temperatures from 20 to 205 °C for 15 minutes.

The identifications of the phase composition of films and calculations of the parameters of the unit cell were performed by X-ray diffractometry (XRD) using a DRON-4-07 (CuKα radiation and Ni filter, 40 kV, 18 mA) at 2Θ = 5–50º, a step of 0.04º and a count time of 4 s.

SiO_2 (angle standard 2Θ) and Al_2O_3 (certified intensity standard) were used as standards [13]. The parameters of the unit cell and the coordinates of atoms were determined using the FullProf program developed by Juan Rodríguez-Carvajal, Laboratoire Léon Brillouin (France) [14].

Peculiarities of phase transformations in the formation of organic-inorganic perovskite $MAPbI_3$ in DMF, DMSO solvents. Plots of the percentage of crystalline phases versus the film treatment temperature were constructed based on diffractograms of perovskite films obtained at different ratios of starting reagents in the DMF solvent (Fig. 1).

Figure 1 shows that the temperature ranges of the existence of intermediate compounds $(MA)_2(DMF)_2Pb_3I_8$, $(MA)_2(DMF)_xPbI_4$, $(MA)_3(DMF)PbI_5$, $(MA)_2(DMF)_2Pb_2I_6$ and organic-inorganic perovskite $MAPbI_3$ in the film can be determined depending on the ratio of reagents. The structure of $MAPbI_3$ perovskite begins to form at a temperature of 20-25 °C, regardless of the ratio of starting reagents. The formation of organic-inorganic perovskite occurs by the formation and decomposition of various amounts of intermediate compounds. At the ratio of starting reagents PbI_2:MAI – 1:1, there are three intermediate compounds, and at 1:2, 1:3 four and two intermediate compounds, respectively. In a detailed analysis of the percentage of crystalline phases and diffractograms, formation reactions of $MAPbI_3$ perovskite were obtained at the PbI_2:MAI = 1:1 ratio in DMF (Table 1).

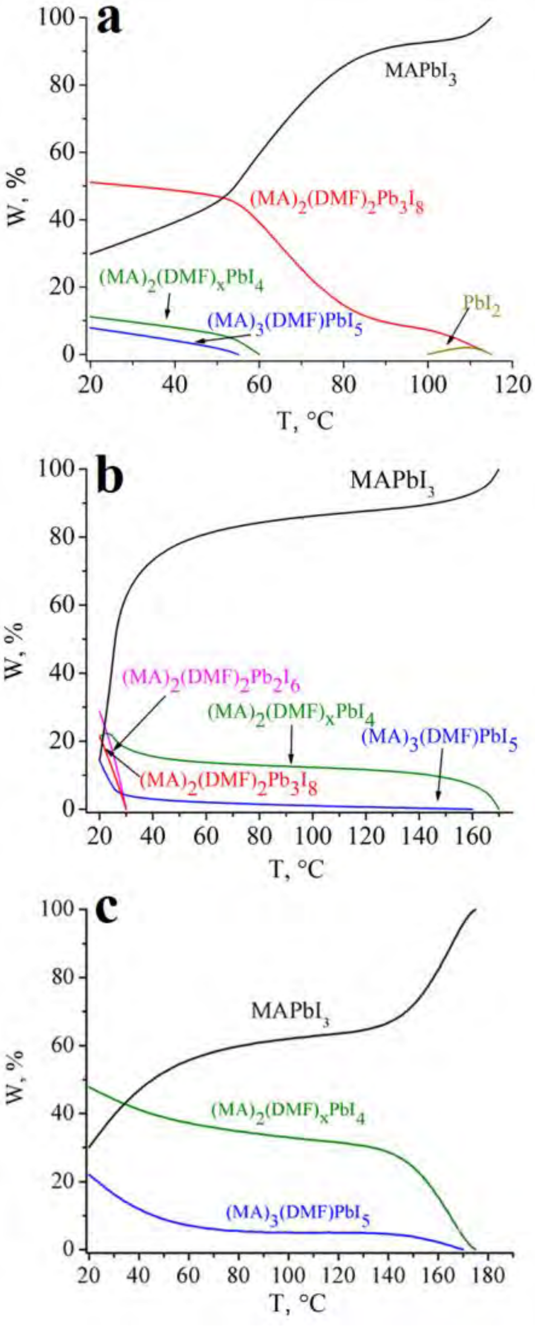

Fig. 1. The dependence of the percentage of crystalline phases on the treatment temperature of the film obtained at different ratios PbI_2:MAI in DMF: a) 1:1; (b) 1:2; (c) 1:3.

Table 1

Phase transformations in the formation of $MAPbI_3$ perovskite at a ratio of starting reagents of 1:1 in DMF.

Reagents	Temperature	Reaction products
$13PbI_2 + 13MAI$ **(1:1 in DMF)**	20–45 °C	$(MA)_3(DMF)PbI_5 + (MA)_2(DMF)_xPbI_4 + 2MAPbI_3 + 3(MA)_2(DMF)_2Pb_3I_8$
	50 °C	$0.5(MA)_3(DMF)PbI_5 + 0.75(MA)_2(DMF)_xPbI_4 + 1.25MAI + 3(MA)_2(DMF)_2Pb_3I_8 + 2.75MAPbI_3$
	55°C	$0.5(MA)_2(DMF)_xPbI_4 + 2.5(MA)_2(DMF)_2Pb_3I_8 + 2MAI + 5MAPbI_3$
	> 55–105 °C	$(MA)_2(DMF)_2Pb_3I_8 + 10MAPbI_3 + MAI$
	>105–110 °C	$0.5(MA)_2(DMF)_2Pb_3I_8 + 11MAPbI_3 + MAI + 0.5PbI_2$
	> 110–115 °C	$13\ MAPbI_3$
$13PbI_2 + 13MAI$	20–45° C	$(MA)_3(DMF)PbI_5 + (MA)_2(DMF)_xPbI_4 + 2MAPbI_3 + 3(MA)_2(DMF)_2Pb_3I_8$
$(MA)_3(DMF)PbI_5$	50 °C	$0.5(MA)_3(DMF)PbI_5 + 0.5(MA)_2(DMF)_xPbI_4 + 0.5MAI + (0.5\text{-}0.5x)DMF$
$2(MA)_2(DMF)_xPbI_4$		$0.25(MA)_2(DMF)_xPbI_4 + 0.75MAPbI_3 + 0.75MAI + 1.5xDMF$
$0.5(MA)_3(DMF)PbI_5$	55 °C	$0.5(MA)_2(DMF)_xPbI_4 + 0.5MAI + (0.5\text{-}0.5x)DMF$
$0.75(MA)_2(DMF)_xPbI_4$		$0.75MAPbI_3 + 0.75MAI + 0.75xDMF$
$3(MA)_2(DMF)_2Pb_3I_8 + 0.5MAI$		$2.5(MA)_2(DMF)_2Pb_3I_8 + 1{,}5MAPbI_3 + 2DMF$
$0.5(MA)_2(DMF)_xPbI_4$	>55-105 °C	$0.5MAPbI_3 + 0.5MAI + 0.5xDMF$
$2.5(MA)_2(DMF)_2Pb_3I_8 + 0.5MAI$		$(MA)_2(DMF)_2Pb_3I_8 + 4.5MAPbI_3 + 3DMF$
$(MA)_2(DMF)_2Pb_3I_8$	> 105–110 °C	$0.5(MA)_2(DMF)_2Pb_3I_8 + MAPbI_3 + 0.5PbI_2 + DMF$
$0.5(MA)_2(DMF)_2Pb_3I_8 + 0.5MAI$	> 110–115 °C	$1{,}5MAPbI_3 + DMF$
$0.5PbI_2 + 0.5MAI$		$0.5MAPbI_3$

At a ratio of 1:1, a single-phase perovskite film is formed at 115 °C. There is a gradual decomposition of the intermediate compound $(MA)_3(DMF)PbI_5$ into $(MA)_2(DMF)_xPbI_4$, which completely decomposes into $MAPbI_3$ at T> 55 °C. The compound $(MA)_2(DMF)_2Pb_3I_8$ is completely decomposed into $MAPbI_3$ perovskite at T> 110 °C.

When the ratio of starting reagents is 1:2 in DMF, a single-phase $MAPbI_3$ perovskite film is formed at 170 °C (Table 2). At this ratio, similar transformations of the intermediate compounds $(MA)_3(DMF)PbI_5$, $(MA)_2(DMF)_xPbI_4$, $(MA)_2(DMF)_2Pb_3I_8$ are observed for the ratio 1:1, but the temperatures of transformations are greatly different. In addition, the conversion of the intermediate $(MA)_2(DMF)_2Pb_2I_6$ to $MAPbI_3$ is observed in this system at T> 30 °C.

Table 2

Phase transformations in the formation of $MAPbI_3$ perovskite at a ratio of starting reagents of 1:2 in DMF.

Reagents	Temperature	Reaction products
$24PbI_2 + 48MAI$ **(1:2 in DMF)**	20 °C	$4(MA)_2(DMF)_2Pb_2I_6 + 2(MA)_3(DMF)PbI_5 + 20MAI + 3(MA)_2(DMF)_xPbI_4 + 3(MA)_2(DMF)_2Pb_3I_8 + 2MAPbI_3$
	25 °C	$3(MA)_2(DMF)_2Pb_2I_6 + (MA)_3(DMF)PbI_5 + 20MAI + 4(MA)_2(DMF)_xPbI_4 + 2(MA)_2(DMF)_2Pb_3I_8 + 7MAPbI_3$
	>30–130 °C	$3(MA)_2(DMF)_xPbI_4 + 0.5(MA)_3(DMF)PbI_5 + 20MAI + 20.5MAPbI_3$
	>130–160 °C	$2.5(MA)_2(DMF)_xPbI_4 + 21.5MAPbI_3 + 21.5MAI$
	>160–170 °C	$24MAPbI_3 + 24MAI$
$24PbI_2 + 48MAI$	20 °C	$4(MA)_2(DMF)_2Pb_2I_6 + 2(MA)_3(DMF)PbI_5 + 3(MA)_2(DMF)_xPbI_4 + 3(MA)_2(DMF)_2Pb_3I_8 + 2MAPbI_3 + 20MAI$
$4(MA)_2(DMF)_2Pb_2I_6$	25 °C	$3(MA)_2(DMF)_2Pb_2I_6 + 2MAPbI_3 + 2DMF$
$2(MA)_3(DMF)PbI_5$		$(MA)_3(DMF)PbI_5 + (MA)_2(DMF)_xPbI_4 + MAI + (1\text{-}x)DMF$
$3(MA)_2(DMF)_2Pb_3I_8 + MAI$		$2(MA)_2(DMF)_2Pb_3I_8 + 3MAPbI_3 + 2DMF$
$3(MA)_2(DMF)_2Pb_2I_6$	>30–130 °C	$6MAPbI_3 + 6DMF$
$(MA)_3(DMF)PbI_5$		$0.5(MA)_3(DMF)PbI_5 + 0.5(MA)_2(DMF)_xPbI_4 + 0.5MAI + (0.5\text{-}0.5x)DMF$
$4(MA)_2(DMF)_xPbI_4$		$2.5(MA)_2(DMF)_xPbI_4 + 1.5MAPbI_3 + 1.5MAI + 1.5xDMF$
$2(MA)_2(DMF)_2Pb_3I_8 + 2MAI$		$6MAPbI_3 + 4DMF$
$3(MA)_2(DMF)_xPbI_4$	>130–160 °C	$2(MA)_2(DMF)_xPbI_4 + MAPbI_3 + MAI + xDMF$
$0.5(MA)_3(DMF)PbI_5$		$0.5(MA)_2(DMF)_xPbI_4 + 0.5MAI + (0.5\text{-}0.5x)DMF$
$2.5(MA)_2(DMF)_xPbI_4$	>160–170 °C	$2.5MAPbI_3 + 2.5MAI + 2.5xDMF$

Table 3

Phase transformations in the formation of $MAPbI_3$ perovskite at a ratio of starting reagents of 1:3 in DMF.

Reagents	Temperature	Reaction products
$9PbI_2 + 27MAI$ **(1:3 in DMF)**	20–150 °C	$4(MA)_2(DMF)_xPbI_4 + (MA)_3(DMF)PbI_5 + 4MAPbI_3 + 12MAI$
	>150–170 °C	$2(MA)_2(DMF)_xPbI_4 + 7MAPbI_3 + 16MAI$
	>170–175 °C	$9MAPbI_3 + 18MAI$
$9PbI_2 + 27MAI$	20–150 °C	$4(MA)_2(DMF)_xPbI_4 + (MA)_3(DMF)PbI_5 + 4MAPbI_3 + 12MAI$
$4(MA)_2(DMF)_xPbI_4 + (MA)_3(DMF)PbI_5$	>150–170 °C	$2(MA)_2(DMF)_xPbI_4 + 4MAI + 3MAPbI_3 + (2x+1)DMF$
$2(MA)_2(DMF)_xPbI_4$	>170–175 °C	$2MAPbI_3 + 2MAI + 2xDMF$

At the ratio PbI_2:MAI = 1:3, the formation of a single-phase $MAPbI_3$ perovskite film occurs at 175 °C (Table 3).

There is a gradual decomposition of the intermediate compound $(MA)_3(DMF)PbI_5$ into 4MAI and $(MA)_2(DMF)_xPbI_4$; the latter completely decomposes into $MAPbI_3$ at T> 170 °C.

Thus, the ratio of starting reagents in DMF significantly affects the number of intermediate compounds that are formed during the synthesis. As the ratio of reagents increases, the temperature of formation of single-phase $MAPbI_3$ perovskite film increases. The $MAPbI_3$ phase is present in the film after heat treatment at 20 °C in amounts of 15-30 wt. %. However, at higher temperatures of 40-60 °C, the intermediate phases begin to decompose, and in this temperature range, the transformation of the intermediate phases into perovskite is not completed.

For the perovskite films synthesized at different ratios of starting reagents in the DMSO solvent, plots of the crystalline phase content versus the film treatment temperature were constructed (Fig. 2).

Figure 2 shows that the structure of $MAPbI_3$ perovskite begins to form at 60 °C for the ratios 1:1, 1:2, and at 70 °C for the ratio 1:3. At a ratio of 1:1, the perovskite film obtained at T> 160 °C begins to degrade, which is accompanied by a decrease in the percentage of perovskite $MAPbI_3$ and an increase in the percentage of the intermediate PbI_2·DMSO (Fig. 2a). At this ratio of starting reagents, a single-phase film is not formed. At a ratio of 1:2, 1:3, intermediate compounds completely decompose and a single-phase $MAPbI_3$ film is formed at 190 and 205 °C, respectively.

The quantitative content of the phases $(MA)_2(DMSO)_2Pb_3I_8$, $(MA)_2(DMSO)_xPbI_4$, PbI_2·DMSO, PbI_2·2DMSO, and organic-inorganic perovskite $MAPbI_3$ in the film depends on the ratio of reagents and treatment temperature.

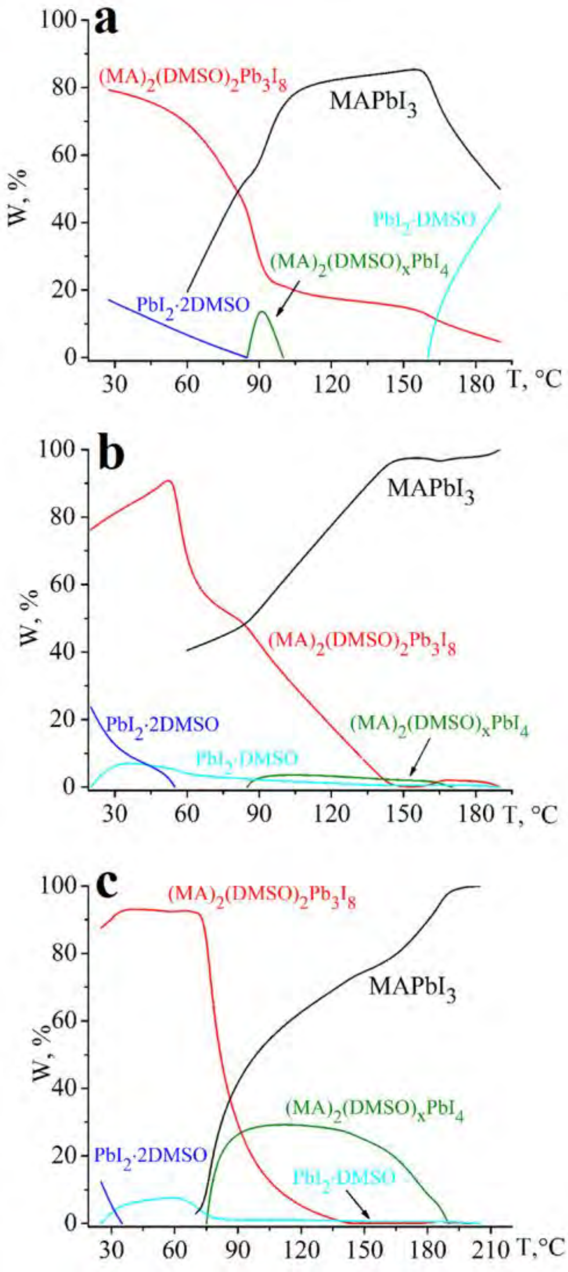

Fig. 2. The dependence of the percentage of crystalline phases on the treatment temperature of the film obtained at different ratios PbI_2:MAI in DMSO: (a) 1:1; (b) 1:2; (c) 1:3.

Table 4

Phase transformations in the formation of $MAPbI_3$ perovskite at a ratio of starting reagents of 1:1 in DMSO.

Reagents	Temperature	Reaction products
$10PbI_2 + 10MAI$ **(1:1 in DMSO)**	20–50 °C	$3(MA)_2(DMSO)_2Pb_3I_8 + PbI_2 \cdot 2DMSO + 4MAI$
	60–85 °C	$2(MA)_2(DMSO)_2Pb_3I_8 + PbI_2 \cdot 2DMSO + 3MAPbI_3 + 3MAI$
	90 °C	$(MA)_2(DMSO)_2Pb_3I_8 + (MA)_2(DMSO)_xPbI_4 + 6MAPbI_3$
	> 90–100 °C	$(MA)_2(DMSO)_2Pb_3I_8 + 7MAPbI_3 + MAI$
	110 °C	$0.5(MA)_2(DMSO)_2Pb_3I_8 + 0.5PbI_2 \cdot 2DMSO + MAI + 8MAPbI_3$
	> 110–160 °C	$0.5(MA)_2(DMSO)_2Pb_3I_8 + 8.5MAPbI_3 + 0.5MAI$
	> 165–180 °C	$0.25(MA)_2(DMSO)_2Pb_3I_8 + 9MAPbI_3 + 0.5MAI + 0.25PbI_2 \cdot DMSO$
	190 °C	$0.25(MA)_2(DMSO)_2Pb_3I_8 + 7MAPbI_3 + 2.25PbI_2 \cdot DMSO + 2.5MAI$
$10PbI_2 + 10MAI$	20–50 °C	$3(MA)_2(DMSO)_2Pb_3I_8 + PbI_2 \cdot 2DMSO + 4MAI$
$3(MA)_2(DMSO)_2Pb_3I_8 + MAI$	60–85 °C	$2(MA)_2(DMSO)_2Pb_3I_8 + 3\ MAPbI_3 + 2DMSO$
$2(MA)_2(DMSO)_2Pb_3I_8 + 2MAI$	90 °C	$(MA)_2(DMSO)_2Pb_3I_8 + (2\text{-}x)DMSO + (MA)_2(DMSO)_xPbI_4 + 2MAPbI_3$
$PbI_2 \cdot 2DMSO + MAI$		$MAPbI_3 + 2DMSO$
$(MA)_2(DMSO)_xPbI_4$	> 90–100 °C	$MAPbI_3 + MAI + xDMSO$
$(MA)_2(DMSO)_2Pb_3I_8$	110 °C	$0.5(MA)_2(DMSO)_2Pb_3I_8 + MAPbI_3 + 0.5PbI_2 \cdot 2DMSO$
$0.5PbI_2 \cdot 2DMSO + MAI$	> 110–160 °C	$0.5\ MAPbI_3 + 0.5\ MAI + DMSO$
$0.5(MA)_2(DMSO)_2Pb_3I_8 + 0.5MAI$	> 165–180 °C	$0.25(MA)_2(DMSO)_2Pb_3I_8 + 0.5MAPbI_3 + 0.25PbI_2 \cdot DMSO + 0.25DMSO$
$0.25PbI_2 \cdot DMSO + 2MAPbI_3$	190 °C	$2\ MAI + 2.25PbI_2 \cdot DMSO$

In a detailed analysis of diffractograms and the phase content of the film, formation reactions of $MAPbI_3$ perovskite at the ratio PbI_2:MAI = 1:1 in DMSO were obtained (Table 4).

At a ratio of starting reagents of 1:1 in DMSO, the formation of organic-inorganic perovskite $MAPbI_3$ occurs through the formation and decomposition of 4 intermediates $(MA)_2(DMSO)_2Pb_3I_8$, $(MA)_2(DMSO)_xPbI_4$, $PbI_2 \cdot DMSO$, $PbI_2 \cdot 2DMSO$. It was shown that the intermediate compound $(MA)_2(DMSO)_2Pb_3I_8$ at 90 °C decomposes into the compound $(MA)_2(DMSO)_xPbI_4$, from which perovskite formation takes place.

At a ratio of 1:2 in DMSO, a single-phase perovskite film is formed at 190 °C (Table 5). In this case, the same 4 intermediate compounds are also formed, which are formed at a ratio of 1:1.

Table 5

Phase transformations in the formation of $MAPbI_3$ perovskite at a ratio of starting reagents of 1:2 in DMSO.

Reagents	Temperature	Reaction products
$8PbI_2 + 16MAI$ **(1:2 in DMSO)**	20–55 °C	$3(MA)_2(DMSO)_2Pb_3I_8 + PbI_2{\cdot}2DMSO + PbI_2{\cdot} DMSO + 12MAI$
	60–85 °C	$2(MA)_2(DMSO)_2Pb_3I_8 + PbI_2{\cdot}DMSO + MAPbI_3 + 11MAI$
	90–140 °C	$(MA)_2(DMSO)_2Pb_3I_8 + PbI_2{\cdot}DMSO + 3MAPbI_3 + 9MAI + (MA)_2(DMSO)_xPbI_4$
	>140–160 °C	$PbI_2{\cdot}DMSO + 2(MA)_2(DMSO)_xPbI_4 + 5MAPbI_3 + 7MAI$
	165 °C	$0.5(MA)_2(DMSO)_2Pb_3I_8 + 0.5PbI_2{\cdot}DMSO + 5MAPbI_3 + (MA)_2(DMSO)_xPbI_4 + 8MAI$
	>165–185 °C	$0.75(MA)_2(DMSO)_2Pb_3I_8 + 5.25MAPbI_3 + 0.5PbI_2{\cdot}DMSO + 9.25MAI$
	190 °C	$8MAPbI_3 + 8MAI$
$8PbI_2 + 16MAI$	20–55 °C	$2(MA)_2(DMSO)_2Pb_3I_8 + PbI_2{\cdot}2DMSO + PbI_2{\cdot}DMSO + 12MAI$
$PbI_2{\cdot} 2DMSO$	60–85 °C	$PbI_2{\cdot}DMSO + DMSO$
$PbI_2{\cdot} DMSO + MAI$		$MAPbI_3 + DMSO$
$2(MA)_2(DMSO)_2Pb_3I_8 + 2MAI$	90–140 °C	$(MA)_2(DMSO)_2Pb_3I_8 + 2MAPbI_3 + (2\text{-}x)DMSO + (MA)_2(DMSO)_xPbI_4$
$(MA)_2(DMSO)_2Pb_3I_8 + 2MAI$	>140–160 °C	$(MA)_2(DMSO)_xPbI_4 + 2MAPbI_3 + (2\text{-}x)DMSO$
$2(MA)_2(DMSO)_xPbI_4 + PbI_2{\cdot} DMSO$	165 °C	$0.5(MA)_2(DMSO)_2Pb_3I_8 + 0.5PbI_2{\cdot}DMSO + (MA)_2(DMSO)_xPbI_4 + MAI + (x\text{-}0.5)DMSO$
$0.5(MA)_2(DMSO)_2Pb_3I_8 + (MA)_2(DMSO)_xPbI_4$	>165-185 °C	$0.75(MA)_2(DMSO)_2Pb_3I_8 + 0.25MAPbI_3 + 1.25MAI + (x\text{-}0.5)DMSO$
$0.75(MA)_2(DMSO)_2Pb_3I_8 + 1.25MAI$	190 °C	$2.25\ MAPbI_3 + 1.5DMSO + 0.5MAI$
$0.5PbI_2{\cdot} DMSO + 0.5MAI$		$0.5MAPbI_3 + 0.5DMSO$

At a ratio of 1:2, interconversion of compounds $(MA)_2(DMSO)_2Pb_3I_8 \leftrightarrow (MA)_2(DMSO)_xPbI_4$ is observed. At low temperatures (90-160 °C) the preceding reaction proceeds in the forward direction with the formation of $(MA)_2(DMSO)_xPbI_4$, while a part of $(MA)_2(DMSO)_2Pb_3I_8$ is converted into $MAPbI_3$. At T > 165-185 °C, the reaction proceeds in the reverse direction, while a part of $(MA)_2(DMSO)_xPbI_4$ is converted into $MAPbI_3$. A conversion of the compound $PbI_2{\cdot}2DMSO$ to $PbI_2{\cdot}DMSO$ is also observed, which in interaction with MAI forms perovskite $MAPbI_3$.

When increasing the ratio of starting reagents to 1:3, a single-phase perovskite film is formed at 205 °C (Table 6). The formation of perovskite occurs through the formation and decomposition of 4 intermediate compounds. At a ratio of 1:3, interconversion of compounds $(MA)_2(DMSO)_2Pb_3I_8 \leftrightarrow (MA)_2(DMSO)_xPbI_4$ is also observed, but in a wider temperature range. There is also a conversion of the compound $PbI_2{\cdot}2DMSO$ to $PbI_2{\cdot}DMSO$, which when interacting with MAI forms perovskite $MAPbI_3$ as for the ratio 1:2.

Table 6

Phase transformations in the formation of $MAPbI_3$ perovskite at a ratio of starting reagents of 1:3 in DMSO.

Reagents	Temperature	Reaction products
$8PbI_2 + 24MAI$ **(1:3 in DMSO)**	20–30 °C	$2(MA)_2(DMSO)_2Pb_3I_8 + PbI_2{\cdot}2DMSO + PbI_2{\cdot}DMSO + 20MAI$
	>30–65 °C	$2(MA)_2(DMSO)_2Pb_3I_8 + 2PbI_2{\cdot}DMSO + 20MAI$
	70–75 °C	$2(MA)_2(DMSO)_2Pb_3I_8 + PbI_2{\cdot}DMSO + MAPbI_3 + 19MAI$
	80–140 °C	$(MA)_2(DMSO)_2Pb_3I_8 + PbI_2{\cdot}DMSO + 3MAPbI_3 + (MA)_2(DMSO)_xPbI_4 + 17MAI$
	>140–160 °C	$3(MA)_2(DMSO)_xPbI_4 + 5MAPbI_3 + 13MAI$
	>165–185 °C	$0.5(MA)_2(DMSO)_2Pb_3I_8 + 0.5(MA)_2(DMSO)_xPbI_4 + 6MAPbI_3 + 16MAI$
	>185–200 °C	$PbI_2{\cdot}DMSO + 7MAPbI_3 + 17MAI$
	205 °C	$8MAPbI_3 + 16MAI$
$8PbI_2 + 24MAI$	20–30 °C	$2(MA)_2(DMSO)_2Pb_3I_8 + PbI_2{\cdot}2DMSO + PbI_2{\cdot}DMSO + 20MAI$
$PbI_2{\cdot}2DMSO + PbI_2{\cdot}DMSO$	>30–65 °C	$2PbI_2{\cdot}DMSO + DMSO$
$2PbI_2{\cdot}DMSO + MAI$	70–75 °C	$PbI_2{\cdot}DMSO + MAPbI_3 + DMSO$
$2(MA)_2(DMSO)_2Pb_3I_8 + 2MAI$	80–140 °C	$(MA)_2(DMSO)_2Pb_3I_8 + 2MAPbI_3 + (2\text{-}x)DMSO + (MA)_2(DMSO)_xPbI_4$
$(MA)_2(DMSO)_2Pb_3I_8 + 3MAI$	>140–165 °C	$MAPbI_3 + 2(MA)_2(DMSO)_xPbI_4 + (2\text{-}2x)\ DMSO$
$PbI_2{\cdot}DMSO + MAI$		$MAPbI_3 + DMSO$
$3(MA)_2(DMSO)_xPbI_4$	>165-185 °C	$0.5(MA)_2(DMSO)_2Pb_3I_8 + MAPbI_3 + 3MAI + 0.5(MA)_2(DMSO)_xPbI_4 + (2.5x\text{-}1)\ DMSO$
$0.5(MA)_2(DMSO)_2Pb_3I_8 + 0.5(MA)_2(DMSO)_xPbI_4$	>185-200 °C	$PbI_2{\cdot}DMSO + MAPbI_3 + MAI + 0.5xDMSO$
$PbI_2{\cdot}DMSO + MAI$	205 °C	$MAPbI_3 + DMSO$

Thus, regardless of the ratio of starting reagents in DMSO, the formation of MAPbI$_3$ perovskite occurs through the formation of 4 intermediate compounds. When the ratio of reagents increases, the temperature of formation of single-phase MAPbI$_3$ film increases.

Crystallographic and electrophysical characteristics of organic-inorganic perovskites MAPbI$_3$, obtained at different ratios PbI$_2$:MAI in DMF, and DMSO. The calculation of the unit cell parameters of organic-inorganic MAPbI$_3$ perovskite films was performed by the Rietveld full-profile analysis method using X-ray diffraction patterns (Fig. 3).

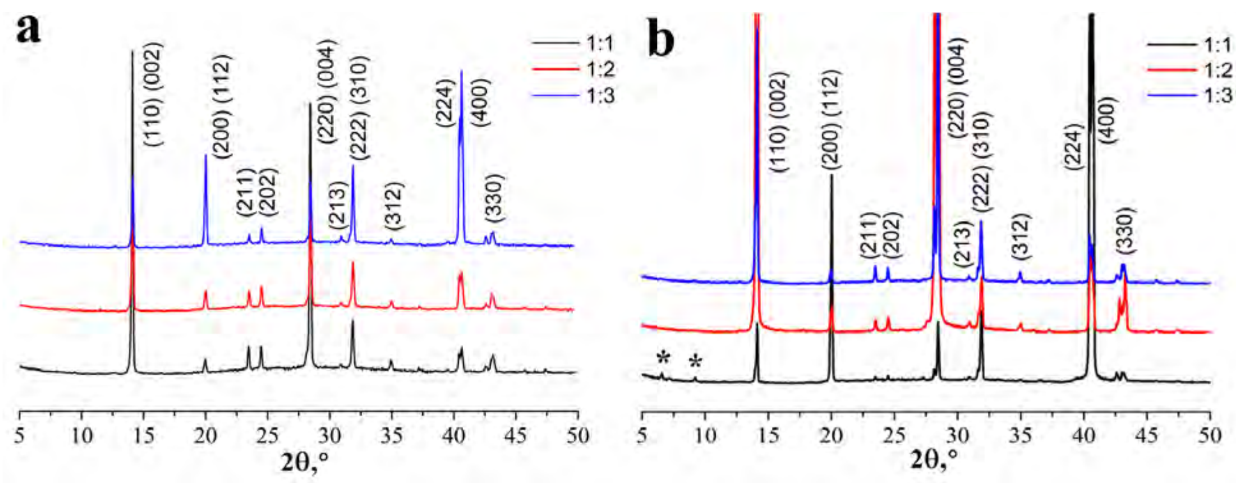

Fig. 3. Experimental X-ray diffraction patterns of samples of MAPbI$_3$ films obtained at different ratios of starting reagents in the DMSO solvent. The Miller indices are given in parentheses. * – $(MA)_2(DMSO)_2Pb_3I_8$.

It was found that depending on the ratio of starting reagents and solvent, there are slight changes in the volume of the cell for perovskite films (Table 7). The changes in the unit cell volume are associated with a small amount of the solvent that is part of the crystalline structure of perovskite. It was proved that the solvent DMSO can replace the cation MA$^+$ in the structure of organic-inorganic perovskite MAPbI$_3$ [15]. The radius of DMSO and DMF molecules are 3.05 Å and 3.13 Å, respectively [16], and the radius of the cation MA$^+$ is 2.17 Å [17]. Since DMF and DMSO molecules are close in size, it can be assumed that DMF enters into the crystal structure, creating deformations. To test this assumption, we will calculate the changes in volume and solvent concentration.

From literature, it is known that the volume of the unit cell for perovskite is $V_{perovskite}$ = 990 Å^3 [18], or $V_{perovskite}/Z = 990/4 = 247.5$ Å^3. Table 7 shows that the experimental values of unit cell volume are slightly larger than the theoretical value of unit cell volume of 990 Å^3.

Table 7

Structural parameters of organic-inorganic perovskites $MAPbI_3$, obtained at different ratios PbI_2:MAI (1:1, 1:2, 1:3) in the DMF and DMSO solvents.

Parameters	DMF			DMSO		
	1:1	1:2	1:3	1:1	1:2	1:3
V, Å^3	994.5(3)	998.6(5)	997.5(4)	991.3(1)	994.7(4)	994.5(2)
Deposition temperature	115 °C	170 °C	175 °C	150 °C	190 °C	205 °C

The calculation of the amount of solvent in the structure of perovskite was performed according to formula (1) using the unit cell volumes of the starting reagents, and perovskite, as well as the volumes of DMF, DMSO solvent molecules, and methylammonium cation MA^+:

$$\frac{V_{perovskite}}{Z_1} = \frac{V_{(PbI_2)}}{Z_2} + \frac{V_{(MAI)}}{Z_3} + (V_{solvent} - V_{(MA^+)}) \cdot x \ , \qquad (1)$$

where Z_1, Z_2, and Z_3 are the formula unit for perovskite, PbI_2, and MAI, respectively, *x* is the amount of solvent included in the structure of perovskite, $V(PbI_2)$ is the unit cell volume of PbI_2, V(MAI) is the unit cell volume of MAI, $V_{solvent}$ is the volume of the solvent molecule, V (MA^+) is the volume of the methylammonium cation MA^+. Taking into account the values of the volumes of compounds and their formula units, we obtain $V(PbI_2)/Z_2 = 125.69/1 = 125.69$ Å^3, $V(MAI)/Z_3 = 235.93/2 = 117.965$ Å^3,

The calculation of the volume of the solvent $(V_{solvent})$ was performed according to formula (2) under the assumption that the solvent molecule has a spherical shape [18].

$$V = \frac{4}{3}\pi R^3 \ , \qquad (2)$$

where R is the radius of the solvent molecule. A similar volume calculation was performed for the MA^+ cation. The volume of the DMF and DMSO solvents is $V_{(DMF)} = 128.4$ Å^3, and $V_{(DMSO)} = 118.8$ Å^3, respectively. The volume of the cation MA^+ is V $(MA^+) = 42.8$ Å^3.

The replacement of a smaller MA^+ cation with a larger molecule of DMF or DMSO leads to minor changes in structural and electrophysical characteristics, which is confirmed by the following calculations.

The solvent content of the structure (x) was determined from formula (3), which was derived from formula (1):

$$x = \frac{\frac{V_{perovskite}}{Z_1} - \frac{V_{(PbI_2)}}{Z_2} - \frac{V_{(MAI)}}{Z_3}}{V_{solvent} - V_{(MA^+)}} \ . \qquad (3)$$

The results of the calculations are summarized in table 8.

Table 8

Determination of the amount of solvent in the structure of perovskite depending on the ratios of starting reagents PbI_2:MAI in the DMF, DMSO solvent.

PbI_2:MAI	$V_{perovskite}$. Å^3	Z_1	$V_{perovskite}/Z_1$. Å^3	$V_{solvent}$. Å^3		x. %
$MAPbI_3$	990.0	4	247.5	–	–	0
1:1	991.3(1)	4	247.8	DMSO	118.8	5.5
1:2	994.7(4)	4	248.7			6.6
1:3	994.5(2)	4	248.6			6.5
1:1	994.5(3)	4	248.6	DMF	128.4	5.8
1:2	998.6(5)	4	249.6			7.0
1:3	997.5(4)	4	249.4			6.7

It was found that at the same ratios of starting reagents, the structure of perovskite included the DMF solvent in a greater amount than DMSO.

The fact that the solvent is part of the structure of perovskite affects not only the structural parameters but also the electrophysical characteristics, in particular, the width of the bandgap (Table 9).

Table 9

Influence of the solvent on the electrophysical characteristics of perovskite $MAPbI_3$.

Solvent		DMF			DMSO		
PbI_2:MAI		1:1	1:2	1:3	1:1	1:2	1:3
Solvent content, %	0	5.8	7	6.7	5.5	6.6	6.5
Bandgap, eV	1.55 [18]	1.59	1.62	1.57	1.57	1.53	1.54

The bandgap for the perovskites obtained at different ratios of starting reagents in DMSO is less than for the films obtained using DMF.

CONCLUSIONS

The peculiarities of formation and properties of organic-inorganic $MAPbI_3$ perovskite films have been studied as a function of the ratio of starting reagents in DMF and DMSO solvents. As the PbI_2:MAI ratio increases, the temperature of the formation of single-phase $MAPbI_3$ perovskite film increases. It was found that when using the DMF solvent, the number of crystalline phases in the film depends on the ratio of starting reagents. At a ratio of 1:1 in DMF, the number of phases is 4 and at 1:2, 1:3 5, and 3, respectively. When using DMSO, regardless of the ratio of starting reagents, there are 5 crystalline phases in the film.

Plots of the percentage of crystalline phases in the film versus the treatment temperature have been constructed for perovskite films synthesized at different ratios of starting reagents in the DMF, and DMSO solvents. It was shown that the formation of organic-inorganic perovskite occurs through the formation and decomposition of intermediate compounds (phases). Reactions of $MAPbI_3$ perovskite formation at different ratios PbI_2:MAI in DMF and DMSO have been obtained.

It was found that for the perovskite films obtained at different ratios PbI_2: MAI in DMF and DMSO, there are slight changes in the structural (unit cell volume) and electrophysical (bandgap) characteristics. These changes are related to the solvent that is included in the crystalline structure of perovskite. It was found that at the same ratios of starting reagents, DMF is included in the structure of perovskite in a greater amount than DMSO.

Acknowledgment. The authors express their gratitude to the Armed Forces of Ukraine for providing security to perform this work. This work has become possible only because of the fortitude and courage of the Ukrainian Army.

ВПЛИВ РОЗЧИННИКА ТА СПІВВІДНОШЕННЯ ВИХІДНИХ РЕАГЕНТІВ НА ВЛАСТИВОСТІ ОРГАНО-НЕОРГАНІЧНОГО ПЕРОВСЬКІТУ $MAPbI_3$

Торчинюк П. В.[1], В’юнов О. І.[1], Власюк В. М.[2], Костильов В. П.[2], Білоус А. Г.[1]

[1]Інститут загальної та неорганічної хімії ім. В. І. Вернадського НАН України, просп. Академіка Палладіна, 32/34, Київ, 03142, Україна
[2]Інститут фізики напівпровідників імені В. Є. Лашкарьова НАН України, просп. Науки, 41, Київ, 03028, Україна
** e-mail: vyunov@ionc.kiev.ua*

Синтезовано органо-неорганічний перовськіт $MAPbI_3$ ($CH_3NH_3PbI_3$) методом одностадійного осадження за різного співвідношення вихідних реагентів (PbI_2 та MAI, які брали у співвідношенні 1:1, 1:2, 1:3) у розчиннику ДМФА та ДМСО. Для отримання плівок органо-неорганічного перовськіту $MAPbI_3$ використовували метод spin-coating.

Досліджено особливості утворення та властивості плівок органо-неорганічного перовськіту $MAPbI_3$ залежно від співвідношення вихідних реагентів у розчиннику DMF, DMSO. Зі збільшенням співвідношення PbI_2:MAI зростає температура утворення однофазної плівки перовськіту $MAPbI_3$. Показано, що утворення органо-неорганічного перовськіту відбувається через утворення та розкладання проміжних сполук (фаз). Отримано реакції утворення перовськіту $MAPbI_3$ за різного співвідношення PbI_2:MAI у DMF, DMSO.

Встановлено, що структура перовськіту $MAPbI_3$ починає формуватися за температури 20–25 °C незалежно від співвідношення вихідних реагентів у DMF. При використанні DMSO структура перовськіту $MAPbI_3$ починає формуватися за температури 60 °C для співвідношень 1:1, 1:2, та при 70 °C для співвідношення 1:3.

Встановлено, що при використанні розчинника DMF кількість кристалічних фаз у плівці залежить від співвідношення вихідних реагентів. При співвідношенні 1:1 у DMF кількість фаз становить 4, а при 1:2, 1:3 – 5 та 3 відповідно. При використанні DMSO незалежно від співвідношення вихідних реагентів у плівці присутні 5 кристалічних фаз.

Для плівок перовськіту, отриманих за різного співвідношення вихідних реагентів у розчиннику DMF, DMSO, було побудовано залежність вмісту кристалічних фаз у плівці від температури оброблення. Встановлено, що для плівок перовськіту, отриманих за різного співвідношення PbI_2:MAI у DMF, DMSO спостерігаємо незначні зміни в структурних (об’єм елементарної комірки) та електрофізичних (ширина забороненої зони) характеристиках. Ці зміни пов’язані з розчинником, який входить у кристалічну структуру перовськіту. Встановлено, що за однакових співвідношень вихідних реагентів DMF входить в структуру перовськіту у більшій кількості, ніж DMSO.

Ключові слова: органо-неорганічний перовськіт, фазові перетворення, структурні параметри, електрофізичні характеристики.

REFERENCES

1. Yang Z., Zhang S., Li L., Chen W., Research progress on large-area perovskite thin films and solar modules. *Journal of Materiomics.* 2017. **3** (4). 231–244.
2. Jiang Q., Zhao Y., Zhang X., Yang X., Chen Y., Chu Z., Ye Q., Li X., Yin Z., You J., Surface passivation of perovskite film for efficient solar cells. *Nature photonics.* 2019. **13** (7). 460–466.
3. Zheng X., Chen B., Dai J., Fang Y., Bai Y., Lin Y., Wei H., Zeng X. C., Huang J., Defect passivation in hybrid perovskite solar cells using quaternary ammonium halide anions and cations. *Nature Energy.* 2017. **2** (7). 1–9.
4. Stolterfoht M., Wolff C. M., Márquez J. A., Zhang S., Hages C. J., Rothhardt D., Albrecht S., Burn P. L., Meredith P., Unold T., Neher D., Visualization and suppression of interfacial recombination for high-efficiency large-area pin perovskite solar cells. *Nature Energy.* 2018. **3** (10). 847–854.
5. Miyata A., Mitioglu A., Plochocka P., Portugall O., Wang J. T.-W., Stranks S. D., Snaith H. J., Nicholas R. J., Direct measurement of the exciton binding energy and effective masses for charge carriers in organic–inorganic tri-halide perovskites. *Nature Physics.* 2015. **11** (7). 582–587.
6. Saba M., Quochi F., Mura A., Bongiovanni G., Excited state properties of hybrid perovskites. *Accounts of Chemical Research.* 2016. **49** (1). 166–173.
7. Han T. H., Tan S., Xue J., Meng L., Lee J. W., Yang Y., Interface and Defect Engineering for Metal Halide Perovskite Optoelectronic Devices. *Advanced Materials.* 2019. **31** (47). 1803515.
8. Zhou Y., Zhao Y., Chemical stability and instability of inorganic halide perovskites.

Energy & Environmental Science. 2019. **12** (5). 1495–1511.

9. Arain Z., Liu C., Yang Y., Mateen M., Ren Y., Ding Y., Liu X., Ali Z., Kumar M., Dai S., Elucidating the dynamics of solvent engineering for perovskite solar cells. *Science China Materials.* 2018. **62** (2). 161–172.
10. Jung M., Ji S.-G., Kim G., Seok S. I., Perovskite precursor solution chemistry: from fundamentals to photovoltaic applications. *Chemical Society Reviews.* 2019. 48 (7). 2011–2038.
11. Kostylyov V. P., Sachenko A. V., Sokolovskyi I. O., Vlasiuk V. M., Torchyniuk P. V., V'yunov O. I., Belous A. G., Shkrebtii A. I., Influence of the reagents' ratio on photoelectric and optical properties of perovskite films for photovoltaics. *Semiconductor Physics, Quantum Electronics and Optoelectronics.* 2021, **24** (3). 295–303.
12. Torchyniuk P. V., V'yunov O. I., Kovalenko L. L., Ishchenko A. A., Kurdyukova I. V., Belous A. G., Influence of Solvent on Stability and Electrophysical Properties of Organic–Inorganic Perovskites Films $CH_3NH_3PbI_3$. *Theoretical and Experimental Chemistry.* 2021. **57** (2). 113–120.
13. Mei A., Li X., Liu L., Ku Z., Liu T., Rong Y., Xu M., Hu M., Chen J., Yang Y., Gratzel M., Han H., A hole-conductor-free, fully printable mesoscopic perovskite solar cell with high stability. *Science.* 2014. **345** (6194). 295–8.
14. Tress W., Marinova N., Moehl T., Zakeeruddin S. M., Nazeeruddin M. K., Grätzel M., Understanding the rate-dependent J–V hysteresis, slow time component, and aging in $CH_3NH_3PbI_3$ perovskite solar cells: the role of a compensated electric field. *Energy & Environmental Science.* 2015. **8** (3). 995–1004.
15. Certificate of Analysis. Standard Reference Material 1976, Instrument Sensitivity Standard for X-ray Powder Diffraction. National Institute of Standards & Technology, Gaithersburg. 1991. 1–4.
16. McCusker L., Von Dreele R., Cox D., Louer D., Scardi P., Rietveld refinement guidelines. *Journal of Applied Crystallography.* 1999. **32** (1). 36–50.
17. Tan Q., Hinrichs K., Mao-Dong H., Fengler S., Rappich J., Prajongtat P., Nickel N. H., Dittrich T., Temperature Dependent Diffusion of DMSO in $CH_3NH_3PbI_3$ Precursor Films During Layer Formation and Impact on Solar Cells. *ACS Applied Energy Materials.* 2019. **2** (7). 5116–5123.
18. Matsuura N., Umemoto K., Takeda Y., Formulation of stokes' radii in DMF, DMSO and propylene carbonate with solvent structure cavity size as parameter. *Bulletin of the Chemical Society of Japan.* 1975. **48** (8). 2253–2257.
19. Kieslich G., Sun S., Cheetham A. K., An extended Tolerance Factor approach for organic-inorganic perovskites. *Chem Sci.* 2015. **6** (6). 3430–3433.
20. Ansari M. I. H., Qurashi A., Nazeeruddin M. K., Frontiers, opportunities, and challenges in perovskite solar cells: A critical review. *Journal of Photochemistry and Photobiology C: Photochemistry Reviews.* 2018. **35.** 1–24.

Стаття надійшла 18.05.2022.